Modulation of Folding and Assembly of the Membrane Protein Bacteriorhodopsin by Intermolecular Forces within the Lipid Bilayer†

A. Rachael Curran,‡ Richard H. Templer,§ and Paula J. Booth*,‡

Departments of Biochemistry and Chemistry, Imperial College for Science, Technology and Medicine, London SW7 2AY, U.K.

Received September 28, 1998; Revised Manuscript Received May 11, 1999

ABSTRACT: Three different lipid systems have been developed to investigate the effect of physicochemical forces within the lipid bilayer on the folding of the integral membrane protein bacteriorhodopsin. Each system consists of lipid vesicles containing two lipid species, one with phosphatidylcholine and the other with phosphatidylethanolamine headgroups, but the same hydrocarbon chains: either L-α-1,2-dioleoyl, L-α-1,2-dipalmitoleoyl, or L-α-1,2-dimyristoyl. Increasing the mole fraction of the phosphatidylethanolamine lipid increases the desire of each monolayer leaflet in the bilayer to curve toward water. This increases the torque tension of such monolayers, when they are constrained to remain flat in the vesicle bilayer. Consequently, the lateral pressure in the hydrocarbon chain region increases, and we have used excimer fluorescence from pyrene-labeled phosphatidylcholine lipids to probe these pressure changes. We show that bacteriorhodopsin regenerates to about 95% yield in vesicles of 100% phosphatidylcholine. The regeneration yield decreases as the mole fraction of the corresponding phosphatidylethanolamine component is increased. The decrease in yield correlates with the increase in lateral pressure which the lipid chains exert on the refolding protein. We suggest that the increase in lipid chain pressure either hinders insertion of the denatured state of bacterioopsin into the bilayer or slows a folding step within the bilayer, to the extent that an intermediate involved in bacteriorhodopsin regeneration is effectively trapped.

Membrane-bound proteins probably account for 30−40% of all cell proteins, yet relatively little is known about the structure, function, and dynamics of these proteins. Similarly, there is only limited information about the molecular details of membrane biogenesis and how the constituent proteins insert into the membrane and fold to achieve a functional state. Here, we focus on the role of the lipids in membrane protein folding.

A major difficulty in the study of membrane proteins lies in finding appropriate detergent or lipid systems that maintain the structural and functional integrity of the protein. This is highlighted in refolding studies where appropriate solubilization conditions must be found to both unfold and refold the protein and, at the same time, prevent aggregation of the often highly hydrophobic proteins. As a result, only a handful of membrane proteins have been refolded in vitro from a denatured state (*1*−*3*). There is, however, a wealth of information available about the structure and dynamics of biological lipids. We hope to exploit this knowledge and, through a systematic manipulation of the lipid environment, to understand the key properties of the lipid systems that govern protein folding events within biological membranes.

Biological membranes contain a diverse group of lipids, with most membranes containing a mixture of "bilayer" and "nonbilayer" forming lipids. It has been suggested that the mix of nonbilayer and bilayer lipids has a generic, functional importance (*4*−*6*) by allowing fine-tuning of certain bilayer properties that seem to be under homeostatic control in living membranes and vital for the correct function of several of the constituent membrane proteins. The introduction of a nonbilayer, type II, lipid into a lipid bilayer increases the desire for the polar−apolar interface of each constituent monolayer to curve toward water. However, the monolayers wish to bend in opposite directions, which they cannot do in a bilayer structure. Thus, there is an increase in the monolayer bending moment, or torque tension, as they are forced to lie flat. This is accompanied by an increase in the lateral pressure in the center of the bilayer due to the increase in the number of collisions between the lipid hydrocarbon chains. We have previously presented evidence that such an increase in the lateral pressure within the bilayer may be responsible for the slowing of a rate-limiting folding step for bacteriorhodopsin (*7*). This previous study used a two-component lipid mixture consisting of lipids with phosphatidylcholine (PC)[1] headgroups but different chain lengths: L-α-1,2-dihexanoylphosphatidylcholine (DHPC, six carbons) and L-α-1,2-dimyristoylphosphatidylcholine (DMPC, 14 carbons). Increasing the amount of the longer chain 14-carbon lipid increases the lateral pressure in the chain region and the bending rigidity of the bilayer. Increasing the bilayer bending rigidity in this manner by about a factor of 2 caused an approximate 10-fold slowing of a rate-limiting folding step of bacteriorhodopsin. Thus, it appeared to be possible to control the rate of protein folding. Our aim is to understand the molecular origin of this control. Unfortunately, although

† This work was supported by The Wellcome Trust (Grant 049763) and The Royal Society. A.R.C. was the recipient of a Postgraduate Bursary from the Department of Biochemistry, Imperial College. P.J.B. is the Rosenheim Research Fellow of the Royal Society.

* To whom correspondence should be addressed.

‡ Department of Biochemistry.

§ Department of Chemistry.

10.1021/bi982322+ CCC: $18.00
Published on Web 06/26/1999

the mixed DMPC/DHPC lipid system gives a qualitative indication that bilayer lateral pressure may alter this folding rate, it is not an ideal system for quantifying this effect. The different chain lengths of the lipids mean that compositional differences alter the hydrophobic thickness of the bilayer. This can result in additional contributions to the lipid lateral pressure. For example, when the bilayer is thinner than the hydrophobic thickness required by the protein, the bilayer will be stretched to avoid hydrophobic mismatch and this will alter the lateral pressure in the chain region (*6*). In addition, the DMPC/DHPC mixtures form bilayer-type, discoidal, mixed micelles. Not only are there additional constraints on the lipid dynamics and pressures as a result of the micellar structure, but also the exact nature of these mixed micelles at different lipid compositions is unknown.

Here, we present the development of a novel refolding system for bacteriorhodopsin that overcomes the problems highlighted above, and in addition allows us to work toward a more biologically relevant situation. Bacteriorhodopsin is refolded directly into lipid vesicles. This has only previously been achieved for β-barrel membrane porins (*8*), as opposed to the rather more hydrophobic, α-helical membrane proteins. Bacteriorhodopsin has previously been regenerated in lipid vesicles, containing either its native *Halobacteria* lipids or soybean, DMPC, or DPPC lipids (*1*, *9*). In these studies, the denatured protein [usually in sodium dodecyl sulfate (SDS)] was first refolded into lipid/detergent mixtures (usually a micellar system) and the detergent then dialyzed away over many hours to form the protein-containing vesicles. We show that it is not necessary to introduce another detergent into the system, and that SDS-denatured bacteriorhodopsin refolds directly on mixing with lipid vesicles. To begin to mimic certain properties of natural membranes, we have used bilayer (PC) and nonbilayer (PE) lipids, with the vesicles consisting of two lipids of the same chain length but with different PC or PE headgroups. The introduction of the smaller PE headgroup increases the intrinsic desire for the monolayer to curve toward the water and thus the lateral pressure in the chain region. To correlate changes in the lipid lateral pressure with protein folding, we apply a recently developed method using pyrene-labeled PC lipids to probe the change in lateral pressure (*10*−*12*).

Bacteriorhodopsin, the proton pump from *Halobacterium salinarium* (*13*), provides an ideal model system for this study. An essential feature for the work is the ability to refold the protein in vitro. Of the very few membrane proteins for which this has been accomplished, there is probably the most information regarding the folding (*1*, *14*−*18*), structure (*19*−*21*), and function (*22*−*25*) for bacteriorhodopsin. The protein consists of a bundle of seven transmembrane α-helices and binds a retinal chromophore covalently within this helical bundle, which gives the protein its characteristic purple color. The regeneration of the purple chromophore provides a good indication of the extent of refolding to a native-like, monomeric, functional state (*1*, *14*). The regeneration kinetics in mixed micelles have been determined with millisecond time resolution following stopped flow mixing of SDS-denatured protein and mixed DMPC/CHAPS or DMPC/DHPC micelles (*26*). There are several kinetic phases associated with this refolding. A key stage in the process appears to be rate-limiting folding to an intermediate with native-like secondary structure, and to which the retinal chromophore binds. This rate-limiting folding step may reflect packing of previously formed helices within the hydrophobic bilayer interior, or insertion of helical segments into the bilayer (*27*). It is this rate-limiting step that can be slowed by 1 order of magnitude by altering the relative amounts of DMPC and DHPC, and thus the lateral pressure in the lipid chain region.

EXPERIMENTAL PROCEDURES

Materials. All phospholipids were obtained from Avanti Phospholipids (Alabaster, AL); dipyrenyl phospholipids were from Molecular Probes, Inc. (Eugene, OR), and *all-trans*-retinal and SDS (electrophoresis grade) were from Sigma. All other chemicals and reagents were of analytical grade.

Bacteriorhodopsin was isolated from purple membranes from *H. salinarium* (strain S9) according to the method of Oesterhelt and Stoeckenius (*28*). Denatured bacterioopsin in SDS was prepared from purple membranes by organic solvent extraction (*29*) as described previously (*30*).

All procedures and measurements were performed at 25.0 ± 0.5 °C for vesicles containing DOPC/DOPE and DPoPC/DPoPE, and at 38.0 ± 0.5 °C for vesicles containing DMPC/DMPE to exceed the gel to fluid (L_β to L_α) phase transition temperature. Small-angle X-ray diffraction and polarizing optical microscopy have shown that at these temperatures all lipid compositions studied here are in a homogeneous fluid, L_α phase (*4*, *31*) .

Lipid vesicles were prepared by dissolving the required lipid composition in a minimum volume of chloroform. The chloroform was then removed in vacuo using either a freeze-dryer or a rotary evaporator. The lipids were then rehydrated with sodium phosphate buffer (50 mM, pH 6), giving a lipid concentration of 2% (w/w). The resulting lipid suspension was then extruded 10 times at 25 °C (or 38 °C for DMPC/DMPE vesicles) through 50, 100, or 200 nm polycarbonate membranes. The resulting lipid vesicles were stored at 25 °C (or 38 °C for DMPC/DMPE vesicles). In all experiments, the buffer that was used was filtered through 0.2 μm cellulose acetate filters before being added to the lipids. For lateral pressure measurements, vesicle preparation was the same except the dipyrenyl probes were added in cyclohexane before solvent evaporation at a probe mole fraction of 0.001.

Mixed DMPC/CHAPS micelles were prepared by stirring 2% (w/v) DMPC in 50 mM sodium phosphate buffer (pH 6) for 2 h at room temperature. CHAPS was then added to a final concentration of 2% (w/v) and the mixture sonicated in a bath for 30 min. The resulting clear micellar solution was then stored at 4 °C for several days.

Dynamic Light Scattering. Vesicle sizes were determined by photon correlation spectroscopy using a Coulter N4 plus

[1] Abbreviations: CHAPS, 3-[(3-cholamidopropyl)dimethylammonio]-1-propanesulfonate; DMPC, L-α-1,2-dimyristoylphosphatidylcholine; DHPC, L-α-1,2-dicaproylphosphatidylcholine; DMPE, L-α-1,2-dimyristoylphosphatidylethanolamine; DOPC, L-α-1,2-dioleoylphosphatidylcholine; DOPE, L-α-1,2-dioleoylphosphatidylethanolamine; DPoPC, L-α-1,2-dipalmitoleoylphosphatidylcholine; DPoPE, L-α-1,2-dipalmitoleoylphosphatidylethanolamine; DPPC, L-α-1,2-dipalmitoylphosphatidylcholine; 10 dipyrenylPC, 1,2-bis(1-pyrenyldecanoyl)-L-α-phosphatidylcholine; *E*, excimer fluorescence; fwhm, full width half-maximum; M_1, lower-wavelength monomer fluorescence band of pyrene; PC, phosphatidylcholine; PE, phosphatidylethanolamine; SDS, sodium dodecyl sulfate.

submicron particle sizer. Vesicle size distributions were determined from the autocorrelation function of light scattered by the vesicles using a weight distribution. This analysis determines the relative weights of different sized vesicles in a given sample. To optimize detection of a broad range of particle sizes, scattered light was detected at angles of 90.0, 62.5, and 23.0° for 300 s at each angle (although shorter detection times are possible at the larger detection angles of 90.0 and 62.5°). The same results were obtained for each detection angle. Vesicles were prepared as described previously and diluted 20 times with 50 mM sodium phosphate buffer (pH 6). All DPoPC/DPoPE vesicles were found to have a homogeneous population with a diameter of 50−55 nm for at least 20 h at 25 °C. Thus, all measurements were taken within 20 h of extrusion.

Steady-State Spectroscopy. Absorption spectra were recorded with a Varian Carey 1G UV/vis spectrophotometer with a 2 nm bandwidth and variable path lengths. Measurements of vesicle samples were recorded using a 1 mm path length cell and an integrating sphere (however, the measurement of bacteriorhodopsin in DMPC/CHAPS with 50 nm DPoPC vesicles in tandem was recorded without the sphere to accommodate the two samples). The protein concentration was between 5 and 7 μM, giving approximately 6−10 proteins per 50 nm vesicle. Studies at different protein concentrations as well as the comparison with DMPC/CHAPS samples showed no evidence of protein−protein interactions or absorption flattening. All other absorption measurements were recorded using a 1 cm path length cell. Fluorescence spectra were recorded using a Spex FluoroMax-2 spectrometer. Intrinsic protein fluorescence was measured by exciting at 290 nm with excitation and emission bandwidths of 2.5 nm. The fluorescence intensity is the area under the intrinsic protein fluorescence band. Pyrene fluorescence was measured by exciting at 342 nm with excitation and emission bandwidths of 1 nm. The fluorescence intensity is the intensity at a particular wavelength: 377 nm for M_1 monomer fluorescence and 475 nm for excimer fluorescence (E). The temperature was controlled at 25.0 ± 0.5 °C for vesicles containing DOPC/DOPE and DPoPC/DPoPE, and 38.0 ± 0.5 °C for vesicles containing DMPC/DMPE for all absorption and fluorescence measurements.

Analysis of Absorption Data and Determination of Regeneration Yields. To monitor both the protein and retinal absorption bands, spectra were measured from 250 to 700 nm. However, only data from 305 to 700 nm were analyzed to obtain the yield of regenerated bacteriorhodopsin as spectra over this range could be collected using only the visible lamp. Data were analyzed by the sum of Gaussian distributions, a Rayleigh function, and on offset using MicroCal Origin and an iterative procedure. The light scattering from the lipid vesicles was approximated to a Rayleigh function of λ^{-4}. Rayleigh scattering assumes that the scattering particles are spherical, uniform in size, and significantly smaller than the wavelength of the incident light. This approximation was found to be reasonable for 50 nm vesicles even at the lower wavelength of 305 nm. The absorption bands of bound and unbound retinal were approximated by Gaussian functions which were defined by the maximum and the full width half-maximum (fwhm). Data were analyzed with all parameters free running as well as with the maxima and fwhm of the Gaussian functions constrained. The quality of the fits was assessed by comparing residuals and Gaussian function parameters to those obtained for samples of known absorption bands: retinal alone in lipid vesicles and bacteriorhodopsin regenerated in DMPC/CHAPS samples (see the Results). On this basis, values for the Gaussian maxima and fwhm were constrained within the ranges of 375−385 and

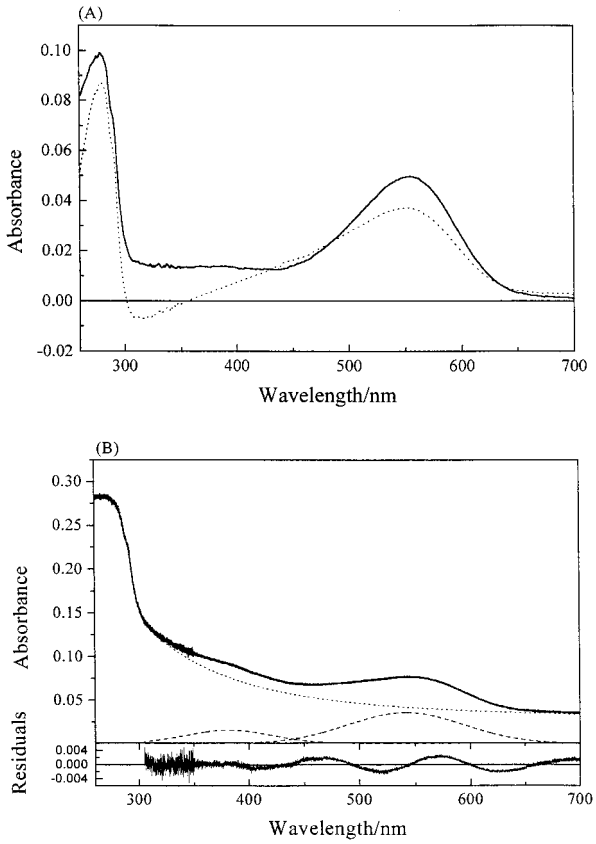

FIGURE 1: Absorption spectra of regenerated bacteriorhodopsin in 50 nm DPoPC vesicles. (A) Absorption spectra of regenerated bacteriorhodopsin in 50 nm DPoPC vesicles (dashed line) with incorrect background correction and in DMPC/CHAPS (solid line) for comparison. Spectra were measured using an integrating sphere which maximizes the collection of scattered light. In both samples, the protein concentration and the yield of regenerated chromophore were the same. Spectra were referenced against the same vesicle or micelle preparation, respectively, that was used in the regeneration experiments, with 0.1% SDS also present in the reference sample. This use of vesicles as a reference resulted in several artifacts in the DPoPC spectrum, including broadening and distortion of the regenerated chromophore band (at ~550 nm), negative absorption features, and a reduction in the intensity of the protein absorption band (at ~280 nm). It is of note that such artifacts can be considerably more subtle than shown here; to highlight the problems, we have deliberately chosen a spectrum with obvious artifacts. (B) Absorption spectrum of regenerated bacteriorhodopsin in 50 nm DPoPC vesicles, referenced against air (solid line) and collected using an integrating sphere. Note that the absorbance scale is different from that in panel A, and the higher absorbance values reflect the light scattering by the vesicles which also contributes to this spectrum. Data were analyzed from 305 to 700 nm by the sum of two Gaussian distributions (dashed line), a Rayleigh function (dotted line), and an offset (with the Gaussian parameters constrained during fitting; see Experimental Procedures). The residuals of the fit are also shown. Such residuals are also typical of fitting a single, well-defined free retinal absorption band in 50 nm DPoPC vesicles to a single Gaussian distribution, Rayleigh function, and offset. The improvements in residuals that can be obtained by allowing all parameters to free run, or by the introduction of a third Gaussian distribution, are due to the Gaussian parameters partly compensating for the light scatter.

55−65 nm, respectively, for unbound retinal and >540 and <110 nm, respectively, for regenerated chromophore. These constraints allow for the slight blue shifting and broadening of the regenerated chromophore absorption band in lipid vesicles compared to those in DMPC/CHAPS micelles, which is due to the difficulty in fully accounting for the light scatter present in the vesicle samples. Typical residuals to the fits are shown in Figure 1b. Better residuals could be obtained with all parameters free running (resulting in further broadening and shifting of the fwhm and Gaussian band maxima), or by the introduction of a third Gaussian distribution. However, such improvements largely represent the Gaussian parameters partly compensating for the light scattering (see the Results). Indeed, the residuals in Figure 1b are similar to those obtained for the well-defined ∼380 nm retinal absorption band of a sample containing only *all-trans*-retinal in lipid vesicles. Unless otherwise stated, all results relate to fits with the Gaussian distributions representing the regenerated chromophore constrained to the values quoted above. Regeneration yields were determined from the extent of recovery of the purple chromophore absorption band. Thus, the area of the Gaussian distribution corresponding to the regenerated chromophore band was calculated. This area was compared to the area of the chromophore band regenerated in DMPC/CHAPS micelles (for the same protein preparation and the same protein concentration as the vesicle sample). The regeneration yield in DMPC/CHAPS was typically about 95%, and was determined from the absorbance at 554.5 nm (*30*).

Regeneration of Bacteriorhodopsin and Determination of Retinal Binding Curves. Bacteriorhodopsin was regenerated in the lipid vesicles from an SDS-denatured state as described previously (*30*) with slight modifications. Bacteriorhodopsin in 0.2% SDS and 50 mM sodium phosphate buffer (pH 6) was mixed in dim red light with an equal volume of lipid vesicles (2% w/v total lipid) containing *all-trans*-retinal (added from an ethanol stock to give a 1:1 molar ratio of retinal to protein). The extent of recovery of the native chromophore absorbance was determined after overnight incubation in the dark at 25 °C. For the retinal binding curves, bacterioopsin in SDS was mixed with the lipid vesicles containing various concentrations of retinal. The yield of regenerated bacteriorhodopsin was determined by a comparison of the relative areas of the regenerated chromophore absorption bands. It should be noted that the error bars are larger than those determined in previous micellar systems due to errors introduced from data fitting to absorption spectra from lipid vesicle samples with highly scattering backgrounds.

SDS Content of Lipid Vesicles. SDS (0.1%) was present in all final lipid vesicle solutions (though not the starting vesicle solution) unless otherwise indicated. The final composition of the lipid vesicles for all regenerated bacteriorhodopsin samples is therefore likely to include some SDS, although the extent of partitioning of the 0.1% SDS present in the sample into the vesicles is unknown. For control measurements without the protein, 0.1% SDS was also present in the final vesicle solution.

RESULTS

Absorption Spectra of Regenerated Bacteriorhodopsin. Bacteriorhodopsin was regenerated from an SDS-denatured state in three different lipid vesicle systems composed of PC and PE lipids: DOPE/DOPE (18-carbon unsaturated chains with a cis double bond between positions C9 and C10), DPoPC/DPoPE (16-carbon unsaturated chains with a cis double bond between positions C9 and C10), and DMPC/DMPE (14-carbon saturated chains). The yield of bacteriorhodopsin regenerated in each lipid vesicle system was determined, as previously reported (*7*, *26*), from the extent of recovery of the native-like purple absorption band, after overnight regeneration in the dark. The lipid vesicles scattered significant amounts of light in the absorption experiments. Figure 1a shows that incorrect subtraction of this light scattering results in spectral artifacts. Light scattering is dependent on vesicle size. Thus, to minimize such problems, small, uniformly sized, 50 nm diameter vesicles were used in the majority of measurements. Vesicles any smaller than this are likely to impose excessive curvature strain on the bilayer. Regeneration yields in larger 100 and 200 nm 100% DPoPC vesicles were the same as in 50 nm vesicles. To obtain a single population of vesicles with a narrow size distribution, vesicles were extruded through 50 nm filters. In addition, absorption spectra of bacteriorhodopsin regenerated in these vesicles were measured using an integrating sphere, which maximizes the collection of scattered light. Nevertheless, subtraction of a reference spectrum of the same vesicle preparation that was used in the regenerated protein sample (with 0.1% SDS present in both samples) still resulted in spectral artifacts (see Figure 1a). This was also true if the reference sample contained protein but, unlike the regenerated protein sample, no retinal. The artifacts are mainly manifested as shifts in absorption band maxima and changes in band intensities. There are two main causes of this. First, the dynamic nature of lipid vesicles means the light scattering changes with time, and second, the protein-containing vesicles appeared to scatter less light than the vesicles alone (SDS being present in both vesicle samples). Bacterioopsin-containing vesicles (with no retinal) also appeared to scatter less light than regenerated bacteriorhodopsin samples. This difference in scattering, together with the fact the light scattering is not synchronized between vesicle samples, means a simple subtraction of a lipid vesicle reference actually increases the noise in the final spectrum by a factor of $\sqrt{2}$, as well as introducing spectral artifacts and the possibility of negative absorption features (see Figure 1a).

Absorption spectra of the 50 nm, protein-containing lipid vesicles were therefore collected with only air or buffer as a reference, and the background light scatter was taken into account during data analysis (Figure 1b). Spectra of regenerated bacteriorhodopsin from 305 to 700 nm were fit to the sum of two Gaussian distributions (representing unbound and bound retinal), a Rayleigh light scattering function, and an offset. For comparison, the same procedure was applied to absorption spectra of bacteriorhodopsin regenerated in DMPC/CHAPS micelles, where the scattering effects are minimal and the absorption bands of the unbound and bound retinal are well defined (*30*). The absorption spectrum of this DMPC/CHAPS sample will be termed spectrum A. Analysis of spectrum A by a sum of Gaussian distributions, a Rayleigh function, and an offset resolved Gaussian parameters for the absorption bands of unbound retinal as 382 nm (fwhm of 62 nm) and of the regenerated chro-

Table 1: Regeneration Yields of Bacteriorhodopsin in Mixed PC/PE Systems[a]

	regeneration yield (%)		
PE mole fraction	DMPC/DMPE	DOPC/DOPE	DPoPC/DPoPE
0.00	94 ± 11	95 ± 15	93 ± 10
0.16	85 ± 14	56 ± 12	62 ± 12

[a] Yields were measured after overnight incubation at 38 °C for DMPC/DMPE and at 25 °C for DOPC/DOPE and DPoPC/DPoPE. DPoPC/DPoPE samples were also incubated and measured at 38 °C and yielded the same result as those measured at 25 °C. Errors are shown to one standard deviation from four measurements with two different protein preparations.

mophore as 552 nm (fwhm of 90 nm), with no other retinal bands (notably at 440 nm; see below) being present. The ability to resolve the well-defined retinal absorption bands in the presence of significant light scattering was also assessed. This was achieved by placing a bacteriorhodopsin, DMPC/CHAPS sample and a 50 nm vesicle sample in the measuring light beam in tandem, but with the two samples in separate cuvettes. The absorption spectrum of this sample will be termed spectrum B. Analysis of spectrum B, with all fitting parameters free running, resolved Gaussian parameters for the free retinal and regenerated chromophore bands as 400 nm (fwhm of 80 nm) and 547 nm (fwhm of 110 nm), respectively. These bands therefore appeared to be broadened and shifted in comparison to the equivalent bands in spectrum A. Spectrum B was also analyzed with the positions and widths of the Gaussian distributions constrained to those resolved for spectrum A. In this case, the results of the fit indicated the need for a third Gaussian distribution with a maximum at approximately 440 nm. However, no such band was present in spectrum A. Thus, the observed broadening and shifting of the retinal absorption bands in spectrum B are effects of the light scatter, rather than of the presence of a third absorbing retinal species at about 440 nm.

Essentially identical behavior was observed for the absorption spectra of bacteriorhodopsin regenerated in all 50 nm PC/PE vesicles that were studied. Thus, in each case the spectra (from 305 to 700 nm) were adequately represented by only two Gaussian distributions reflecting unbound retinal and the regenerated chromophore, with these bands appearing broader and shifted compared to those of bacteriorhodopsin regenerated in DMPC/CHAPS. For example, analyses of spectra of bacteriorhodopsin regenerated in 50 nm vesicles of 100% DPoPC and DPoPC/DPoPE (PE mole fraction of 0.16) gave values of 542 nm (fwhm of 101 nm) and 550 nm (fwhm of 96 nm), respectively. The blue shift in the maximum of the regenerated chromophore band (from 552 nm in DMPC/CHAPS) appears to decrease with an increasing PE component. While this blue shift may have physical significance, it more likely results from a decrease in the regenerated chromophore band intensity with increasing PE (see Table 1 and Figure 2a). Thus, as a result of this lower density of data for the chromophore band, the apparent band shift as a result of light scattering is smaller.

Bacteriorhodopsin Regeneration Yields. The regeneration yield of bacteriorhodopsin was about 95% in all 100% PC systems that were studied. The introduction of PE into the PC vesicles resulted in a marked decrease in regeneration yield (see Table 1). Figure 2a shows the decrease in

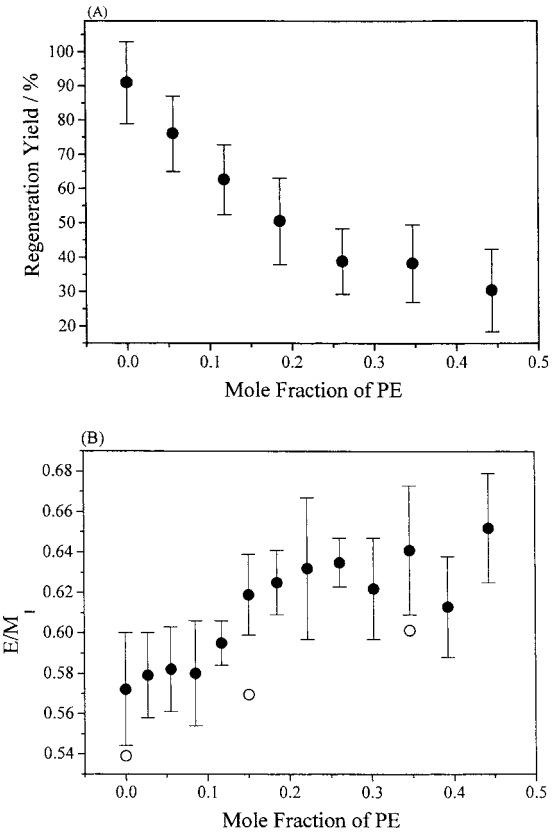

FIGURE 2: Effect of increasing the DPoPE concentration on the regeneration yield of bacteriorhodopsin and the lateral pressure within DPoPC/DPoPE bilayers. (A) Regeneration yield of bacteriorhodopsin in 50 nm DPoPC/DPoPE vesicles as a function of DPoPE composition. Regeneration yields were determined from the extent of recovery of the purple chromophore absorption band after overnight incubation in the dark at 25 °C, as described in Experimental Procedures. Errors are shown to one standard deviation from from measurements with two different protein preparations. (B) Excimer/monomer (E/M_1) ratio of 10 dipyrenylPC in 50 nm DPoPC/DPoPE vesicles (with no SDS present) (●) as a function of DPoPE composition. The same relative change in E/M_1 ratio with PE was observed for DPoPC/DPoPE vesicles where 0.1% SDS was present in the sample. Errors are shown to one standard deviation from four measurements each with a different sample preparation. Also shown are E/M_1 values for 50 nm DOPC/DOPE vesicles (with no SDS present) (○). An increase in the E/M_1 ratio is due to an increase in the lipid chain lateral pressure near the center of the bilayer. Fluorescence spectra were measured at 25 °C. Dipyrenyl probes were incorporated at a mole fraction of 0.001.

regeneration yield as a function of increasing PE concentration in DPoPC/DPoPE vesicles. The amount of unbound retinal (absorption band at 380 nm) also increased systematically with the decrease in the amount of regenerated protein.

The retinal binding curves for regenerating bacteriorhodopsin in 100% DPoPC vesicles and DPoPC/DPoPE vesicles (with a PE mole fraction of 0.19) were determined as described previously (*30*). Figure 3 shows the change in the amount of regenerated chromophore as a function of retinal concentration for both 100% DPoPC and DPoPC/DPoPE (0.19 PE mole fraction). The level of chromophore absorption increases linearly with retinal concentration until a maximum is reached. As previously noted (*7*, *30*), the change in protein fluorescence as a function of retinal concentration mirrors the change observed in regenerated chromophore absorbance. Figure 3a shows that in vesicles composed of 100% DPoPC all of the added retinal binds to

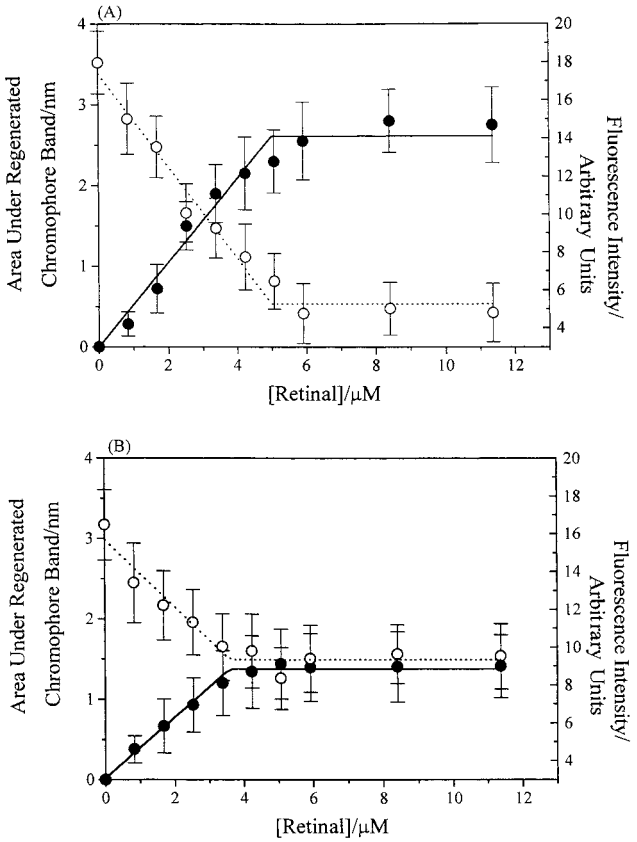

FIGURE 3: Changes in chromophore absorbance and protein fluorescence as a function of retinal concentration, on regeneration of bacteriorhodopsin in DPoPC and DPoPC/DPoPE vesicles. Regeneration of bacteriorhodopsin (A) in 100% DPoPC vesicles and (B) in mixed DPoPC/DPoPE vesicles (PE mole fraction of 0.19): changes in (●) the area under the regenerated chromophore band and (○) the area under the intrinsic protein fluorescence band. The lines through the points are shown as a guide, and represent fits to a tight binding model of one retinal per protein. Each data point represents measurements on separate bO samples (from the same bO preparation), to which retinal was added simultaneously. Errors are shown to one standard deviation from measurements on three different sample preparations, all from the same protein preparation. The protein concentration was 6.2 μM. Samples were measured after overnight incubation at 25 °C.

the protein until the concentration of the added retinal is approximately equal to that of the protein. After this point, almost all the available protein has bound retinal and regenerated bacteriorhodopsin. This is consistent with a regeneration yield of approximately 100% (see Table 1). In the DPoPC/DPoPE system (Figure 3b), however, all the retinal that is added binds to the protein until a maximum is reached when the retinal concentration is approximately equal to 50% of the protein concentration. Again this is consistent with the regeneration yield of 62% reported in Table 1 for DPoPC/DPoPE vesicles with a slightly lower PE mole fraction of 0.16.

Determination of the Lipid Lateral Pressure in the Chain Region. Changes in the lateral pressure of the lipid chains in the vesicles were estimated by incorporating the pyrene-labeled lipid, L-α-1,2-bis(1-pyrenyldecanoyl)phosphatidylcholine (10 dipyrenylPC), into the PC/PE vesicles. This attachment of the pyrenes at position C10 of the lipid chains means the pyrenes are located in the chain region of the membrane from C10 down to the bilayer midpoint, and thus monitor pressure changes around the center of the bilayer.

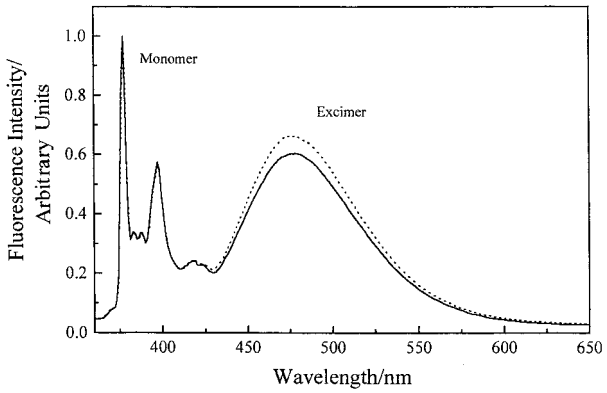

FIGURE 4: Fluorescence spectra of 10 dipyrenylPC in DPoPC and DPoPC/DPoPE vesicles (—) in 100% DPoPC and (•••) in mixed DPoPC/DPoPE vesicles with a PE mole fraction of 0.35. Two sharp monomeric bands, M_1 and M_2, are seen at 377 and 397 nm, respectively, and an excimer band is seen at ~475 nm. Spectra were measured at 25 °C with an excitation wavelength of 342 nm. The fluorescence intensity is normalized to that of the lower-wavelength monomer fluorescence at 377 nm. The higher relative excimer fluorescence in DPoPC/DPoPE vesicles reflects the higher lateral pressure in the hydrocarbon chain region of the bilayer.

Typical fluorescence spectra of 10 dipyrenylPC in both 100% DPoPC vesicles (no SDS present) and DPoPC/DPoPE vesicles (with a PE mole fraction of 0.35 and no SDS present) are shown in Figure 4. Two sharp monomeric bands, M_1 and M_2, are seen at 377 and 397 nm, respectively, and an excimer band is seen at ~475 nm. The excimer is formed when a ground state and excited-state pyrene moieties are in close proximity (~3.5 Å) and of the correct orientation. The ratio of the pyrene excimer to monomer (E/M_1) fluorescence is an effective measure of the lateral pressure of the lipid chains (*11*, *12*, *32*). The greater relative excimer fluorescence in the DPoPC/DPoPE vesicles is due to more collisions between pyrene molecules (on the same lipid molecule), which reflects a greater lateral pressure of the lipid chains. Excimer formation between pyrenes on different labeled lipids is dependent on the pyrene concentration as well as on the lipid lateral pressure. To avoid such intermolecular excimers, the mole fraction of the pyrene-labeled lipid was about 0.001.

Figure 2b shows the increase in the pyrene excimer to monomer (E/M_1) fluorescence as a function of increasing PE concentration in DPoPC/DPoPE and DOPC/DOPE vesicles (with no SDS present). This reflects the increase in lipid chain lateral pressure on the introduction of PE. The same relative change of pyrene excimer to monomer fluorescence on PE concentration was observed for DPoPC/DPoPE vesicles with 0.1% SDS present.

DISCUSSION

Three lipid-based refolding systems have been developed for an investigation into the effect of intermolecular forces within lipid bilayers on the refolding of bacteriorhodopsin. Each system meets two key requirements. First, they allow manipulation of the intermolecular lipid forces through the incorporation of PE lipids into a PC bilayer. This increases both the monolayer torque tension and the lateral pressure of the lipid chains. Second, bacteriorhodopsin can be regenerated from its SDS-denatured apoprotein state to high yield, with a >90% yield of regenerated protein being

obtained in DMPC, DOPC, or DPoPC vesicles. The chromophore absorption band of the dark-adapted, regenerated bacteriorhodopsin in DPoPC vesicles seems to have an absorption maximum at 542 nm, which appears blue shifted compared to that of 554 nm for bacteriorhodopsin previously regenerated in mixed DMPC/CHAPS micelles (*7*, *26*, *30*). However, the chromophore band in DMPC/CHAPS micelles also appears to be blue-shifted to 547 nm in the presence of significant light scattering (see the Results). Thus, the apparent blue shift of the regenerated chromophore band in the DPoPC vesicles is most likely a result of the light scattering from the vesicles. The oscillator strengths of the chromophore absorption bands in DPoPC and DMPC/CHAPS agree to within 12%. The native chromophore is therefore regenerated in DPoPC vesicles, reflecting recovery of native-like bacteriorhodopsin.

A correct match in the hydrophobic thickness of the bilayer and a membrane protein (*6*, *33*) is likely to be important for protein folding. Although there are conflicting literature reports about the magnitude of the hydrophobic thicknesses of the three lipid systems we have investigated (*34*, *35*), the hydrophobic thicknesses of lipid systems probably only differ by about 4 Å, and are little affected by PE content. Any resulting hydrophobic mismatch with bacteriorhodopsin has no effect on the ability of each 100% PC system that was investigated to refold bacteriorhodopsin. Although the introduction of PE is unlikely to change the hydrophobic thickness, it may alter the effective lipid lateral pressure experienced by the protein (see Dependence of Bacteriorhodopsin Regeneration Yield on the Lipid Chain Lateral Pressure).

Our results show that a great deal of caution must be taken when interpreting absorption spectra of lipid vesicle samples that scatter significant amounts of the measuring light. This is an important point for studies of membrane proteins where absorption measurements are routinely made on samples that scatter significant amounts of light, and usually by subtraction of a scattering reference background (generally without an integrating sphere to maximize the scattered light collection). We have shown that such an approach is not valid, and can result in artifactual band shifts, intensity changes, and the introduction of spurious absorption bands.

Dependence of Regeneration Yield on the PE Content of PC/PE Lipid Vesicles. The introduction of PE into DPoPC, DOPC, or DMPC vesicles causes a reduction in the regeneration yield of bacteriorhodopsin (see Table 1 and Figure 2a). The regenerated bacteriorhodopsin in DPoPC/DPoPE vesicles has an absorption maximum at 550 nm and an oscillator strength within 10% of that regenerated in DPoPC vesicles alone. Thus, the protein that does regenerate in DPoPC/DPoPE vesicles exhibits a native-like chromophore. If we assume that retinal binding causes a red shift in the absorption spectrum of retinal from 380 nm, our results also imply that the protein which is unable to regenerate native-like bacteriorhodopsin is also unable to bind retinal. However, due to the light scattering by the vesicles, a red shift of about 10−20 nm of the retinal absorption band (i.e., to 390−400 nm) could not be reliably detected in our measurements. We have previously reported that a transient, 430 nm retinal−protein intermediate is involved in the regeneration of bacteriorhodopsin in DMPC/CHAPS micelles (*36*). Extensive regeneration studies of retinal binding to bacterioopsin in its native membrane environment also reveal noncovalently bound retinal, protein intermediates with absorption maxima at 400 and 430/460 nm (*16*, *37*, *38*). A 440 nm retinal−protein intermediate may be present in the final spectra of bacteriorhodopsin regenerated in the PC/PE systems; however, the noise in the absorption data as a result of background light scattering means that this 440 nm component cannot be accurately resolved (see the Results).

Dependence of Bacteriorhodopsin Regeneration Yield on the Lipid Chain Lateral Pressure. Increasing the mole fraction of the nonbilayer, PE lipid in the mixed PC/PE lipid systems increases the monolayer torque tension and lateral pressure in the lipid chain region (*4*). There is a direct correlation between the regeneration yield of bacteriorhodopsin in PC/PE lipid vesicles and the lateral pressure in the bilayer center (Figure 2). An increase in the lateral pressure of the lipid chains (see Figure 2b) is accompanied by a decrease in the regeneration yield of bacteriorhodopsin (see Figure 2a) for all three regeneration systems that were investigated (see Table 1). A comparison of the two unsaturated DOPC/DOPE and DPoPC/DPoPE systems shows that the dependence of the regeneration yield on the concentration of PE is not equal. Although the increase in lipid chain lateral pressure with increasing PE levels appears to be the same in both vesicle systems (see Figure 2b), a slightly greater decrease in regeneration yield was consistently observed with increasing PE levels in DOPC/DOPE vesicles than in DPoPC/DPoPE vesicles (see Table 1). It should however be noted that the 10 dipyrenylPC measurements used here do not probe the complete lipid chain pressure profile. Furthermore, the hydrophobic thickness of DOPC/DOPE and DPoPC/DPoPE bilayers must differ by approximately 3 Å, which means at least one of these systems is slightly mismatched with respect to the hydrophobic thickness of bacteriorhodopsin. As already discussed (see the introductory section), such hydrophobic mismatches alter the lateral pressure in the region of the protein.

An increase in the monolayer torque tension and lipid chain lateral pressure in PE/PC vesicles appears to impede the regeneration of bacteriorhodopsin. The state of the protein that is unable to regenerate bacteriorhodopsin in PC/PE vesicles is unclear, along with why this protein appears to be unable to bind retinal. Two of the simplest scenarios based on all our data to date are as follows. First (model 1, Figure 5), the protein that does not regenerate bacteriorhodopsin is unable to insert into the lipid membrane and remains partially denatured in SDS micelles. An increase in the monolayer torque tension, as well as in the lipid chain lateral pressure, on addition of PE will make it more difficult for this denatured protein to enter the bilayer. The relatively small amount of SDS used in our experiments is insufficient to release the torque tension enough to allow the protein to insert. However, this is clearly finely balanced since increasing the SDS concentration (from 0.1 to 0.2%, final concentration) shifts the refolding equilibrium to the SDS-denatured protein, thus maintaining a low regeneration yield (results not shown).

The second possible explanation (model 2, Figure 5) is that all of the protein can insert into the lipid membrane; however, not all of the protein is able to fold correctly. We have shown previously that a rate-limiting folding step appears to be slowed by increasing the lipid chain lateral

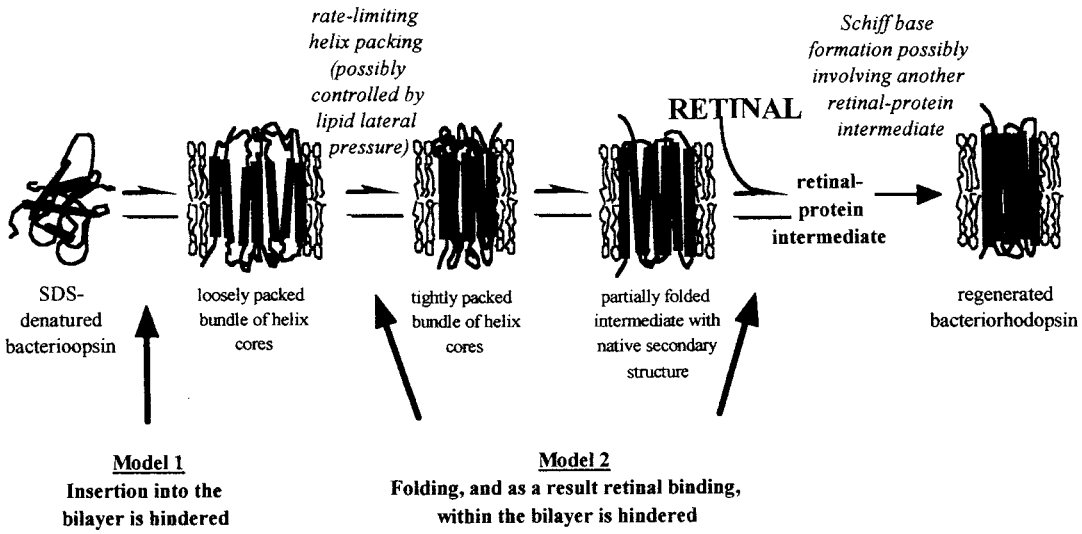

FIGURE 5: Possible steps in the folding and assembly of bacteriorhodopsin that may be modulated by an increase in monolayer torque tension and lipid chain lateral pressure. In model 1, the increase in monolayer torque tension and lipid chain lateral pressure, as PE is introduced into the bilayer, lowers the regeneration yield by hindering insertion into the bilayer. In model 2, the regeneration yield is lowered as a result of the increased lipid chain lateral pressure impeding protein folding and assembly, possibly to the extent of trapping an intermediate in the assembly process. The stages within the bilayer that may be hindered by the increased lipid lateral pressure are a rate-limiting (possible helix packing) step or retinal binding to a partially folded intermediate with native secondary structure where the helix bundle is too tightly packed. The reaction scheme is based on the hypothesis developed for the folding of the protein from studies in DMPC/DHPC micelles (*27*), and is only one possible scheme. Not only may there be additional steps, but also the rate-limiting step could reflect insertion of certain helical segments into the bilayer.

pressure. The introduction of PE into PC vesicles is therefore also likely to result in a slowing of this rate-limiting step, possibly to the extent of effectively trapping a folding intermediate (or allowing a competing reaction which does not lead to functional protein), thus resulting in a lower regeneration yield. Although it is possible that a retinal-bound assembly intermediate is trapped (for example, the 430 nm retinal−protein intermediate), the simplest interpretation of our data thus far is that it is folding prior to retinal binding which is affected by the increase in lipid chain lateral pressure.

In principle, the two models shown in Figure 5 could be distinguished by separating any protein-containing SDS micelles from bacteriorhodopsin-containing lipid vesicles. However, column chromatography cannot be applied, since it will perturb the equilibrium that is being studied. It has also not proved to be possible to separate the two species by density gradient centrifugation or to obtain conclusive results on the relative populations of protein-containing SDS micelles and lipid vesicles from particle sizing by dynamic light scattering or electron microscopy.

The results presented here, together with our previous report (*7*), strongly suggest that the monolayer torque tension and lateral pressure within lipid bilayers can modulate the insertion and folding of membrane proteins. This offers the potential to control specific membrane processes, such as transmembrane helix movement. Furthermore, there is mounting evidence that these lipid intermolecular forces within bilayers play key roles both in vitro and in vivo. The recent novel crystallization method reported for bacteriorhodopsin seems to be dependent on the manipulation of the lipid intermolecular forces (*39*). The introduction of PE into PC bilayers has also been shown to modulate the function of several membrane-bound proteins, including alamethicin (*40*), cytidyl transferase (G. S. Attard, R. H. Templer, W. S. Smith, A. N. Hunt, and S. Jackowski, unpublished observations), rhodopsin (*41*), Ca^{2+}-ATPase (*42*), and lactose permease (*43*). Since helix movements have been shown to be important in the function of rhodopsin (*44*), it therefore seems likely that the increase in the lipid chain lateral pressure, as a result of increasing the PE content, could modulate the function of rhodopsin (and hence the other examples mentioned here) by affecting helix movement. The cell membrane composition of both *Escherichia coli* and *Acholeplasma laidlawii* (*45*, *46*) is also altered in response to their environment. Relative ratios of bilayer and nonbilayer lipids are varied such that the membrane maintains a particular monolayer torque tension, thus presumably optimizing membrane activity.

We have developed efficient refolding systems that allow specific bilayer properties to be altered and the resulting effect on membrane protein folding to be determined. Bacteriorhodopsin is the only α-helical integral membrane protein for which a biophysical study of protein folding events and conformational changes involving transmembrane α-helices is currently possible. The lyotropic properties of the native lipids of purple membranes—phosphatidyl glycerophosphate, phosphatidyl glycerol, sulfonated lipids (glycolipid sulfate and phosphatidyl glycerosulfate), and neutral lipids (e.g., squalenes) (*47*)—have not been studied in detail. Thus, extensively studied PC and PE lipids (which are also major constituents of biological membranes) have been chosen here for the development of a model system. This has allowed us to investigate the generic properties of biological membranes that may modulate protein assembly and function. The fact that bacteriorhodopsin can be refolded to full functionality in PC/PE systems, and its behavior modulated, appears to lend support to the idea that perhaps the precise chemical details of the membrane composition are not as important as the physical pressures that the membrane exerts on the protein. Bilayer lateral pressure and torque tension in particular may be important means of

regulating membrane function which can be exploited as a means of controlling membrane processes.

ACKNOWLEDGMENT

We thank David Klug and Ian Mercer for helpful discussions particularly with regard to data collection and analysis, Louise Riley and Wim Meijberg for assistance with protein preparation and many helpful comments, Ben Hankamer for the electron microscope studies, and Ida Lister for help with dynamic light scattering measurements. We are also grateful to George Attard for the use of a particle sizer and Garry Rumbles for the use of a fluorometer in the initial stages of the work.

REFERENCES

1. Huang, K.-S., Bayley, H., Liao, M.-J., London, E., and Khorana, H. G. (1981) *J. Biol. Chem. 256*, 3802−3809.
2. Eisele, J.-L., and Rosenbusch, J. P. (1990) *J. Biol. Chem. 265*, 10217−10220.
3. Plumley, F. G., and Schmidt, G. W. (1987) *Proc. Natl. Acad. Sci. U.S.A. 84*, 146−150.
4. Seddon, J. M. (1990) *Biochim. Biophys. Acta 1031*, 1−69.
5. Gruner, S. M. (1985) *Proc. Natl. Acad. Sci. U.S.A. 82*, 3665−3669.
6. Bloom, M., Evans, E., and Mouritsen, O. G. (1991) *Q. Rev. Biophys. 24*, 293−397.
7. Booth, P. J., Riley, M. L., Flitsch, S. L., Templer, R. H., Farooq, A., Curran, A. R., Chadborn, N., and Wright, P. (1997) *Biochemistry 36*, 197−203.
8. Surrey, T., and Jähnig, F. (1992) *Proc. Natl. Acad. Sci. U.S.A. 89*, 7457−7461.
9. Popot, J.-L., Gerchman, S.-E., and Engelman, D. M. (1987) *J. Mol. Biol. 198*, 655−676.
10. Cowsley, S. J., Templer, R. H., and Klug, D. R. (1993) *J. Fluoresc. 3*, 149−152.
11. Castle, S. J. (1995) Ph.D. Thesis, Imperial College for Science, Technology and Medicine, London.
12. Templer, R. H., Castle, S. J., Curran, A. R., Rumbles, G. R., and Klug, D. R. (1998) *Faraday Discuss. 111*, 41−53.
13. Oesterhelt, D., and Stoeckenius, W. (1971) *Nat. New Biol. 233*, 149−152.
14. London, E., and Khorana, H. G. (1982) *J. Biol. Chem. 257*, 7003−7011.
15. Liao, M.-J., London, E., and Khorana, H. G. (1983) *J. Biol. Chem. 258*, 9949−9955.
16. Schreckenbach, T., Walckhoff, B., and Oesterhelt, D. (1977) *Eur. J. Biochem. 76*, 499−511.
17. Khorana, H. G. (1988) *J. Biol. Chem. 263*, 7439−7442.
18. Popot, J.-L., and Engelman, D. M. (1990) *Biochemistry 29*, 4031−4037.
19. Pebay-Peyroula, E., Rummel, G., Rosenbusch, J. P., and Landau, E. M. (1997) *Science 277*, 1676−1681.
20. Kimura, Y., Vassylyev, D. G., Miyazawa, A., Kidera, A., Matsushima, M., Mitsuoka, K., Murata, K., Hira, T., and Fujiyoshi, Y. (1997) *Nature 389*, 206−211.
21. Grigorieff, N., Ceska, T. A., Downing, K. H., Baldwin, J. M., and Henderson, R. (1996) *J. Mol. Biol. 259*, 393−421.
22. Oesterhelt, D. (1998) *Curr. Opin. Struct. Biol. 8*, 489−500.
23. Lanyi, J. K. (1998) *J. Biol. Chem. 272*, 31209−31212.
24. Tittor, J. (1993) *Curr. Opin. Struct. Biol. 1*, 534−538.
25. Altenbach, C., Marti, T., Khorana, H. G., and Hubbell, W. L. (1990) *Science 248*, 1088−1092.
26. Booth, P. J., Flitsch, S. L., Stern, L. J., Greenhalgh, D. A., Kim, P. S., and Khorana, H. G. (1995) *Nat. Struct. Biol. 2*, 139−143.
27. Booth, P. J. (1997) *Folding Des. 2*, R85−R92.
28. Oesterhelt, D., and Stoeckenius, W. (1974) *Methods Enzymol. 31*, 667−679.
29. Braiman, M. S., Stern, L. J., Chao, B. H., and Khorana, H. G. (1987) *J. Biol. Chem. 262*, 9271−9276.
30. Booth, P. J., Farooq, A., and Flitsch, S. L. (1996) *Biochemistry 35*, 5902−5909.
31. Rand, R. P., Fuller, N. L., Gruner, S. M., and Parsegian, V. A. (1990) *Biochemistry 29*, 76−87.
32. Kinnunen, P. K. J., Koiv, A., and Mustonen, P. (1993) in *Fluorescence Spectroscopy. New Methods and Applications* (Wolfbeis, O. S., Ed.) Springer-Verlag, Heidelberg, Germany.
33. Piknová, B., Pérochon, E., and Tocanne, J.-F. (1993) *Eur. J. Biochem. 218*, 385−396.
34. Lewis, B. A., and Engelman, D. M. (1982) *J. Mol. Biol. 166*, 211−217.
35. Lis, L. J., McAlister, M., Fuller, N., Rand, R. P., and Parsegian, V. A. (1982) *Biophys. J. 37*, 657−666.
36. Booth, P. J., and Farooq, A. (1997) *Eur. J. Biochem. 246*, 674−680.
37. Schreckenbach, T., Walckhoff, B., and Oesterhelt, D. (1978) *Biochemistry 17*, 5353−5359.
38. Gärtner, W., Towner, P., Hopf, H., and Oesterhelt, D. (1983) *Biochemistry 22*, 2637−2644.
39. Landau, E. M., and Rosenbusch, J. P. (1996) *Proc. Natl. Acad. Sci. U.S.A. 93*, 14532−14535.
40. Keller, S. L., Bezrukov, S. M., Gruner, S. M., Tate, M. W., Vodyanoy, I., and Parsegian, V. A. (1993) *Biophys. J. 65*, 23−27.
41. Gibson, N. J., and Brown, M. F. (1993) *Biochemistry 32*, 2438−2454.
42. Navarro, J., Toivio-Kinnucan, M., and Racker, E. (1984) *Biochemistry 23*, 130−135.
43. Chen, C. C., and Wilson, T. H. (1984) *J. Biol. Chem. 259*, 10150−10158.
44. Farrens, D. L., Altenbach, C., Yang, K., Hubbell, W. L., and Khorana, H. G. (1996) *Science 274*, 768−770.
45. Lindblom, G., and Rilfors, L. (1989) *Biochim. Biophys. Acta 988*, 221−256.
46. Morein, S., Andersson, A., Rilfors, L., and Lindblom, G. (1996) *J. Biol. Chem. 271*, 6801−6809.
47. Kushwaha, S. C., Kates, M., and Martin, W. G. (1975) *Can. J. Biochem. 53*, 284−292.

BI982322+